

Three-body continuum discretization in a basis of transformed harmonic oscillator states

M. Rodríguez-Gallardo^{1,2}, J.M. Arias¹, J. Gómez-Camacho¹, A.M. Moro¹, I.J. Thompson², and J.A. Tostevin²

¹ Departamento de Física Atómica, Molecular y Nuclear, Facultad de Física,
Universidad de Sevilla, Apartado 1065, 41080 Sevilla, Spain and

² Department of Physics, University of Surrey, Guildford GU2 7XH, United Kingdom.

(Dated: 13th August 2018)

The inclusion of the continuum in the study of weakly-bound three-body systems is discussed. A transformed harmonic oscillator basis is introduced to provide an appropriate discrete and finite basis for treating the continuum part of the spectrum. As examples of the application of the method the strength functions corresponding to several operators that couple the ground state to the continuum are investigated, for ${}^6\text{He}$, and compared with previous calculations. It is found that the energy moments of these distributions are accurately reproduced with a small basis set.

PACS numbers: 21.45.+v, 21.10.-k, 27.20.+n, 03.65.Ca

I. INTRODUCTION

The general solution of a quantum mechanical Hamiltonian problem containing a time-independent potential gives rise to both bound and unbound eigenstates. Usually the Hamiltonian of the system has a finite number of bound eigenstates while the unbound ones form a continuum. For the description of nuclei in the stability valley usually only the bound eigenstates are considered. However, the development of radioactive nuclear beam facilities has allowed the study of nuclei far from the line of stability, bringing to the fore new nuclear structure problems. One of the main topics in recent years has been the study of halo nuclei [1, 2]. These are weakly-bound, spatially extended systems, typically comprising a core and one or two valence nucleons.

A particularly interesting example of exotic systems is that of Borromean nuclei, i.e., three-body composite systems with no binary bound states. These nuclei have deserved special attention because their loosely-bound nature reflects a delicate interplay between two- and three-body forces, thus constituting a challenge to existing theories, and a motivation for the development of new ones. Even today, the detailed structure of the continuum spectrum of these systems is not fully understood, partially due to the ambiguities associated with the underlying forces between the constituents. Due to their low binding energy, halo nuclei are easily broken up in the nuclear and Coulomb field of the target. Therefore few-body reaction theories, developed to extract reliable information from experimental data of reactions involving loosely bound systems, have to include, as an essential ingredient, a realistic description of the continuum part of the spectrum.

From the theoretical point of view, the treatment of reactions involving loosely bound systems deals with the complication that breakup states are not square-normalizable. A convenient method to circumvent this problem is to replace the states in the continuum by a finite set of normalized states, thus providing a discrete basis that, hopefully, can be truncated to a small number of states and give a good description of the contin-

uum. Several prescriptions to construct a discrete basis have been proposed. For two-body composite systems, where true continuum states are easily calculated, one can use a discretization procedure in which the continuum spectrum is truncated at a maximum excitation energy and divided into energy intervals. For each interval, or bin, a normalizable state is constructed by superposition of scattering states within that bin interval. The method, known as the Continuum Discretized Coupled Channels (CDCC) method [3, 4], has been very useful in the description of elastic and breakup observables in reactions involving weakly bound two-body projectiles. An alternative method to obtain a discrete representation of the continuum spectrum is to diagonalize the two-body Hamiltonian in a complete set of L^2 functions such as Gaussians [5, 6] or Laguerre functions [7, 8, 9]. This method has the appealing feature of being readily applicable to three-body systems, in which case the Hamiltonian is diagonalized in a complete set of square-integrable functions for the 3-body Hilbert space. Several applications of this method can be found in the literature, for both structure [10] and reaction problems [11]. In the latter case, the method constitutes a natural extension of the CDCC formalism for reactions with three-body projectiles.

When the ground state wave function is already known, a useful procedure to obtain a discrete representation for scattering states consists of performing a Local Scale Transformation (LST) [12] that transforms the ground state wave function of the system into the ground state of a Harmonic Oscillator (HO) [13, 14]. Once the LST is obtained, the HO basis can be transformed by the inverse LST to a discrete basis in the physical space. The functions in the Transformed Harmonic Oscillator (THO) basis are not eigenfunctions of the Hamiltonian (except for the ground state) but the Hamiltonian can be diagonalized in an appropriate truncated basis to produce approximate eigenvalues and eigenfunctions. This method has been shown to be useful for describing the two-body continuum in both structure [13, 14, 15] and scattering [16, 17] problems. In particular, it was shown that global

structure functions, related to the coupling to the continuum, such as strength functions, are very accurately described using a relatively small THO basis.

In this work we extend the THO formalism presented in [13, 14] to treat the three-body continuum. In particular we apply the method to the Borromean nucleus ^6He . This is a very weakly bound system with a well developed structure, of an α cluster and two valence neutrons. Most of our knowledge of this nucleus comes from the analysis of reactions where secondary beams of ^6He collide with stable nuclei. These experiments have been performed with both light [18, 19] and heavy targets [20, 21, 22, 23, 24], and at low and high energies, providing a rich variety of data which can be used to benchmark reaction and structure models.

Theoretically, ^6He has been the object of many studies, using three-body methods [25, 26, 27, 28, 29, 30], cluster-orbital shell models [31, 32], no-core microscopic shell models [33] and microscopic cluster models, and for various effective nucleon-nucleon interactions [34, 35]. In the present work, the three-body equations are solved according to the formalism described in Ref. [25]. In this reference, several three-body methods are compared and applied to the ground state properties of the Borromean nuclei ^6He and ^{11}Li . One of these approaches, discussed in [25], consists of a solution of the Faddeev equations in configuration space. In the Faddeev formalism, the total wave function for a three-body system is expressed as a superposition of three terms, one for each Jacobi configuration. This wave function, which contains both scattering and rearrangement channels, is obtained by solving a set of coupled integro-differential equations. A practical way to solve the problem is to express the three-body wave function in terms of hyperspherical coordinates. For convenience, scattering states are expanded in terms of a discrete basis. In Ref. [25] a family of Gauss-Laguerre functions was used for this purpose. In the present work, we choose a THO basis obtained from a 3-body calculation of the ^6He nucleus.

The method we present can also be used as an input for reaction theories. However, in the present paper we present only results related to the structure of ^6He . In particular, we investigate strength functions for several operators that couple the ^6He ground state to the continuum. Results related to scattering processes induced by ^6He will be presented in a forthcoming paper.

This paper is structured as follows. In Section II the THO formalism for a three-body system is developed. In Section III the formalism is then applied to the case of the structure of ^6He . Finally, Section IV summarizes and draws conclusions from this work.

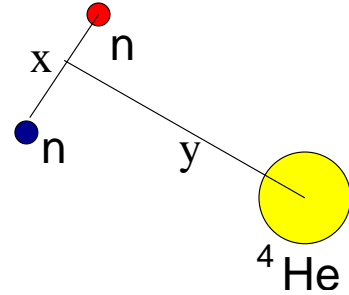


Figure 1: The Jacobi T-coordinate system used to describe the ^6He system.

II. FORMALISM OF THE TRANSFORMED HARMONIC OSCILLATOR (THO) STATES FOR A THREE-BODY CONTINUUM SYSTEM

In this Section we develop the formalism of transformed harmonic oscillator states to be applied to three-body continuum systems. To a large extent, this formalism is a generalization of the method presented in [13, 14]. For such a system we will use the hyperspherical coordinates that are obtained from the Jacobi coordinates (see, for instance, [36]). Consider three particles of masses $\{m_1, m_2, m_3\}$ and whose locations are defined by $\{\mathbf{r}_1, \mathbf{r}_2, \mathbf{r}_3\}$. Three sets of Jacobi coordinates $\{\mathbf{x}_i, \mathbf{y}_i\}$, with $i = 1, 2, 3$, can be defined where $\{\mathbf{x}_i\}$ is the relative coordinate for two particles and $\{\mathbf{y}_i\}$ is the coordinate of the third particle relative to the center of mass of the two particles used to define $\{\mathbf{x}_i\}$:

$$\begin{aligned} \mathbf{x}_i &= (\mathbf{r}_j - \mathbf{r}_k) \sqrt{\frac{\mu_{x_i}}{m}}, \\ \mathbf{y}_i &= \left(\mathbf{r}_i - \frac{m_j \mathbf{r}_j + m_k \mathbf{r}_k}{m_j + m_k} \right) \sqrt{\frac{\mu_{y_i}}{m}}. \end{aligned} \quad (1)$$

Here μ_{x_i} is the reduced mass of the $\{j, k\}$ system and μ_{y_i} is the reduced mass of the $(j + k)$ and particle i system,

$$\begin{aligned} \mu_{x_i} &= \frac{m_j m_k}{m_j + m_k}, \\ \mu_{y_i} &= \frac{m_i (m_j + m_k)}{m_i + m_j + m_k}, \end{aligned} \quad (2)$$

and m is an arbitrary normalization mass that we will take as the nucleon mass. The indices i, j, k run through $(1, 2, 3)$ in cyclic order.

From these Jacobi coordinates, one can introduce the hyperspherical coordinates defined by the hyperradius ρ and the hyperangle α_i ,

$$\begin{aligned} \rho^2 &= x_1^2 + y_1^2 = x_2^2 + y_2^2 = x_3^2 + y_3^2, \\ \tan \alpha_i &= x_i / y_i, \end{aligned} \quad (3)$$

with $x_i = \rho \sin \alpha_i$ and $y_i = \rho \cos \alpha_i$. Note that the hyperangle depends on the Jacobi system selected but not on the hyperradius.

For the three-body system of a core, considered inert and spin-less, plus two valence particles, the total wave

function is assumed to be a product of the core intrinsic wave function $\phi_c(\xi_c)$ and the two-valence-particle plus core relative motion wave function $\Psi_{JM}(1, 2)$. $\Psi_{JM}(1, 2)$ depends on the relative coordinates and the spins of the two particles and is the solution of the Schrödinger equation

$$(\hat{T} + \hat{V} - E)\Psi(1, 2) = 0 \quad (4)$$

with

$$\hat{V} = \hat{V}_{c1} + \hat{V}_{c2} + \hat{V}_{12}. \quad (5)$$

\hat{V}_{ci} is the interaction of the core with particle i and \hat{V}_{12} the interaction between particles 1 and 2.

From this point, we work within the Jacobi T-coordinate system, shown in Fig. 1, and hence all subsequent formulae refer to this coordinate set. Expanding $\Psi_{JM}(1, 2)$ using the hyperspherical harmonics (HH) referred to these coordinates

$$\Psi_{JM}(1, 2) = \sum_{\beta} R_{\beta}(\rho) \left[\Upsilon_{Kl}^{l_x l_y}(\Omega) \otimes X_S \right]_{JM}, \quad (6)$$

where ρ is the hyperradius, $\beta \equiv \{K, l_x, l_y, l, S\}$ labels each channel, $R_{\beta}(\rho)$ is the hyperradial wave function, $\Upsilon_{Kl}^{l_x l_y}(\Omega)$ is a hyperspherical harmonic in the angles $\Omega = (\alpha, \hat{x}, \hat{y})$, and $X_S(1, 2)$ is the total spin wave function of particles 1 and 2. $\mathbf{J} = \mathbf{l} + \mathbf{S}$ is the total angular momentum of the system, since the core particle is assumed spinless. The hyperspherical harmonics are

$$\Upsilon_{Klm_l}^{l_x l_y}(\Omega) = \Psi_K^{l_x l_y}(\alpha) [Y_{l_x}(\hat{x}) \otimes Y_{l_y}(\hat{y})]_{lm_l}, \quad (7)$$

$$\begin{aligned} \Psi_K^{l_x l_y}(\alpha) &= N_K^{l_x l_y} (\sin \alpha)^{l_x} (\cos \alpha)^{l_y} \\ &\times P_n^{l_x+1/2, l_y+1/2}(\cos 2\alpha), \end{aligned} \quad (8)$$

where l_x and l_y are the orbital angular momenta associated with the Jacobi coordinates x and y , respectively, K is the hypermomentum and $P_n^{a,b}$ is a Jacobi polynomial with $n = (K - l_x - l_y)/2$. Usually the hyperradial part is written as $R_{\beta}(\rho) = \rho^{-5/2} U_{\beta}(\rho)$. Then, for bound states $U(\rho) \rightarrow 0$ for $\rho \rightarrow \infty$ with asymptotic behaviour $U(\rho) \rightarrow \exp(-k\rho)$ with $\hbar^2 k^2/2m = -E$.

A. The THO method

The problem is now to solve the Eq. (4) and find its eigenvalues and eigenvectors. For that purpose, one needs a basis in which the Hamiltonian can be diagonalized. As mentioned above, one can expand the channel wave function $\Psi_{\beta JM}(\rho, \Omega)$ in the HH basis as

$$\Psi_{\beta JM}(\rho, \Omega) = R_{\beta}(\rho) \sum_{m_l \sigma} \langle lm_l S \sigma | JM \rangle \Upsilon_{Klm_l}^{l_x l_y}(\Omega) X_S^{\sigma}. \quad (9)$$

$R_{\beta}(\rho)$ is the hyperradial wave function and here we will use the THO method to obtain it. The basic idea of the

THO method is to perform a local scale transformation (LST) of the ground state wave function of the system under study into the harmonic oscillator ground state wave function. We now obtain such a LST for a three-body system. The ground state of the system $\Psi_B(\rho, \Omega)$ is written as a linear combination of the basis functions, Eq. (9),

$$\Psi_B(\rho, \Omega) = \sum_{\beta} R_{B\beta}(\rho) \sum_{m_l \sigma} \langle lm_l S \sigma | J_B \nu \rangle \Upsilon_{Klm_l}^{l_x l_y}(\Omega) X_S^{\sigma}. \quad (10)$$

Consequently, we will obtain a LST for each channel β included in the ground state. This is done by transforming the hyperradial wave function for each channel included in the bound ground state function, $R_{B\beta}(\rho)$, into the corresponding (same K) harmonic oscillator ground state wave function for that channel $R_{0K}^{HO}(s)$. In the six-dimensional case, these functions are

$$R_{iK}^{HO}(s) = N_{iK} s^K L_i^{K+2}(s^2) \exp(-s^2/2) \quad (11)$$

where N_{iK} is the normalization constant

$$N_{iK} = \sqrt{\frac{2\Gamma(i+1)}{\Gamma(i+K+3)}}. \quad (12)$$

Here $L_i^{K+2}(x)$ is a generalized Laguerre polynomial with i the order of the polynomial and which describes the hyperradial excitation. The LST for a given channel β included in the bound ground state is defined by the equation

$$\int_0^{\rho_{\beta}} d\rho \rho^5 |R_{B\beta}(\rho)|^2 = \int_0^s ds' s'^5 |R_{0K}^{HO}(s')|^2. \quad (13)$$

Once the LST for each channel $\rho_{\beta}(s)$ is obtained, the THO basis is defined by applying the inverse transformation $s_{\beta}(\rho)$ to the HO wave functions generated from the corresponding ground state wave function,

$$R_{i\beta}^{THO}(\rho) = \frac{N_{iK}}{N_{0K}} R_{B\beta}(\rho) L_i^{K+2}(s_{\beta}(\rho)^2). \quad (14)$$

Usually, instead of $R_{i\beta}^{THO}(\rho)$, the following hyperradial wave function is introduced

$$U_{i\beta}^{THO}(\rho) = \rho^{5/2} R_{i\beta}^{THO}(\rho) \quad (15)$$

that fulfills the orthonormality relationship

$$\int_0^{\infty} d\rho U_{i\beta}^{THO}(\rho) U_{i'\beta}^{THO}(\rho) = \delta_{ii'}. \quad (16)$$

Thus, we obtain the THO basis

$$\Psi_{i\beta JM}^{THO}(\rho, \Omega) = \rho^{-5/2} U_{i\beta}^{THO}(\rho) \quad (17)$$

$$\times \sum_{m_l \sigma} \langle lm_l S \sigma | JM \rangle \Upsilon_{Klm_l}^{l_x l_y}(\Omega) X_S^{\sigma}. \quad (18)$$

It is easy to show that these states form a complete orthonormal set.

Since the THO basis is infinite, one diagonalizes the Hamiltonian in a finite truncation, obtaining eigenstates

$$\Psi_{nJM}(\rho, \Omega) = \sum_{i\beta} C_{nJM}^{i\beta} \Psi_{i\beta JM}^{THO}(\rho, \Omega) \quad (19)$$

Convergence of the results with the basis truncation must then be checked.

The information available on the different channels included in the ground state wave function allows one to construct the corresponding LST's directly, Eq. (13). For channels not included in the ground state, as a general rule, information from one of the known (ground state) channels with the closest quantum labels to the channel of interest is used to construct the LST. One important point concerns the label K which governs the ρ^K behavior of the hyperradial wave function close to the origin. In order to keep this behavior correct we always select a channel from the ground state wave function with the same K as the channel under study. If this is not possible, a channel with $K - 1$ is used and the corresponding hyperradial wave function is then multiplied by ρ .

So, for example, the hyperradial wave function for $\beta = \{1, 1, 0, 1, 1\}$, $J^\pi = 1^-$ is obtained by multiplying by ρ the wave function for $\beta = \{0, 0, 0, 0, 0\}$, $J^\pi = 0^+$. The wave function for $\beta = \{2, 2, 0, 2, 0\}$, $J^\pi = 2^+$ is taken to be the same as the one for $\beta = \{2, 0, 0, 0, 0\}$, $J^\pi = 0^+$. It is worth noting that $l_x + l_y \leq K$, while for the ground

state components $l_x = l_y$.

B. Hamiltonian matrix elements

Recalling that one set of Jacobi coordinates has been selected $\{\mathbf{x}, \mathbf{y}, \mathbf{R}\}$, and removing the CM contribution, the Hamiltonian is written in hyperspherical coordinates as

$$\widehat{H}(\rho, \Omega) = \widehat{T}(\rho, \Omega) + \widehat{V}(\rho, \Omega) \quad (20)$$

The kinetic energy operator, in the differential equations for the $U(\rho) = \rho^{5/2} R(\rho)$, is

$$\widehat{T}(\rho, \Omega) = -\frac{\hbar^2}{2m} \left[\frac{\partial^2}{\partial \rho^2} + \frac{5}{\rho} \frac{\partial}{\partial \rho} - \frac{1}{\rho^2} \widehat{K}^2(\Omega) \right]. \quad (21)$$

The kinetic energy operator does not connect channels with different β or J , i.e.

$$\begin{aligned} \langle THO; i, \beta, J | \widehat{T} | THO; i', \beta', J' \rangle = \\ \langle THO; i, \beta, J | \widehat{T} | THO; i', \beta, J \rangle \delta_{\beta, \beta'} \delta_{J, J'}, \end{aligned} \quad (22)$$

and hence only matrix elements within these channels have to be calculated. These matrix elements are, with $s_\beta^2 \equiv s_\beta(\rho)^2$,

$$\begin{aligned} \langle THO; i, \beta, J | \widehat{T} | THO; i', \beta, J \rangle = & \frac{N_{iK} N_{i'K}}{N_{0K}^2} \left[\int_0^\infty d\rho \frac{dU_{0\beta}(\rho)^2}{d\rho} L_i^{K+2}(s_\beta^2) L_{i'}^{K+2}(s_\beta^2) \right. \\ & + \int_0^\infty d\rho U_{0\beta}(\rho)^2 L_{i-1}^{K+3}(s_\beta^2) L_{i'-1}^{K+3}(s_\beta^2) \left(2s_\beta(\rho) \frac{ds_\beta(\rho)}{d\rho} \right)^2 \\ & - \int_0^\infty d\rho \frac{dU_{0\beta}(\rho)}{d\rho} U_{0\beta}(\rho) L_{i-1}^{K+3}(s_\beta^2) L_{i'}^{K+2}(s_\beta^2) 2s_\beta(\rho) \frac{ds_\beta(\rho)}{d\rho} \\ & - \int_0^\infty d\rho \frac{dU_{0\beta}(\rho)}{d\rho} U_{0\beta}(\rho) L_i^{K+2}(s_\beta^2) L_{i'-1}^{K+3}(s_\beta^2) 2s_\beta(\rho) \frac{ds_\beta(\rho)}{d\rho} \\ & \left. + \left(\frac{15}{4} + K(K+4) \right) \int_0^\infty d\rho \frac{U_{0\beta j}(\rho)^2}{\rho^2} L_i^{K+2}(s_\beta^2) L_{i'}^{K+2}(s_\beta^2) \right]. \end{aligned} \quad (23)$$

These integrals are evaluated by quadratures.

The potential energy operator connects different channels within the same J . The hyperangular integration is performed using the code FaCE [36] on the set of hyper-

radial quadrature points providing the set of functions $V_{\beta\beta'}^J(\rho)$. The potential energy matrix elements in the THO basis are then simply

$$\langle THO; i, \beta, J | \widehat{V}(\rho, \Omega) | THO; i', \beta', J \rangle = \int_0^\infty d\rho U_{i\beta}^{THO}(\rho) V_{\beta\beta'}^J(\rho) U_{i'\beta'}^{THO}(\rho). \quad (24)$$

The formalism presented above provides a complete basis and the corresponding Hamiltonian matrix elements. In the following Section we apply the method to study ${}^6\text{He}$.

III. STRUCTURE CALCULATION FOR ${}^6\text{HE}$

The ${}^6\text{He}$ nucleus is treated here as a three-body system, comprising an inert α core and two valence neutrons. The ground state has total angular momentum $J^\pi = 0^+$ and an experimental binding energy of 0.973 MeV. The ground state wave function was obtained by solving the Schrödinger equation in hyperspherical coordinates, following the procedure described in [25, 36]. Besides the two-body ($n - n$ and $n - \alpha$) potentials, the model Hamiltonian also includes a simple central hyper-radial three-body force. This is introduced to overcome the under-binding caused by the other closed channels, the most important of which are $t+t$ channels. The $n-{}^4\text{He}$ potential is taken from Ref. [37, 38], with central and spin-orbit components, and the GPT NN potential [39] with central, spin-orbit and tensor components is used. These calculations were performed with the code FaCE [36]. All calculations truncate the maximum hypermomentum at $K_{max} = 20$ and the three-body force is adjusted to give the right binding energy. The calculated three-body wave function has a binding energy of 0.954882 MeV and a rms point nucleon matter radius of 2.557 fm when assuming an alpha-particle rms matter radius of 1.47 fm.

In Fig. 2 we plot the hyperradial parts for the first three channels of the ${}^6\text{He}$ ground state wave function. The labels correspond to the quantum numbers $\{K, l_x, l_y, l, S\}$. These channels give the main contribution to the wave function.

From the ground state, the LST for the different channels are obtained as explained in the preceding section. In Fig. 3 the $s_\beta(\rho)$ for the LST's of the most important ${}^6\text{He}$ ground state channels are shown. The THO basis is constructed from these LST using Eq. (18).

In Fig. 4 the first few hyperradial wave functions for the channel $\beta = \{2, 0, 0, 0, 0\}$, and for $J^\pi = 0^+$, are presented. This is the most important ground state channel, making a 79% contribution to the total norm. We see that as the quantum number i increases the wave functions are more oscillatory and explore larger distances.

With the THO basis one can proceed to calculate the Hamiltonian matrix elements and diagonalize the Hamiltonian matrix in a truncated space. In Fig. 5 the Hamiltonian eigenvalues for $J^\pi = 0^+$, for different maximum values of the hyperradial excitations, n_b , are presented up to $\varepsilon = 10$ MeV. The calculated ground state energy is -0.954886 MeV.

To study different strength functions from the ${}^6\text{He}$ ground state to the three-body continuum, states with different values of J^π have to be generated. Thus, we have to construct a THO basis for these states starting

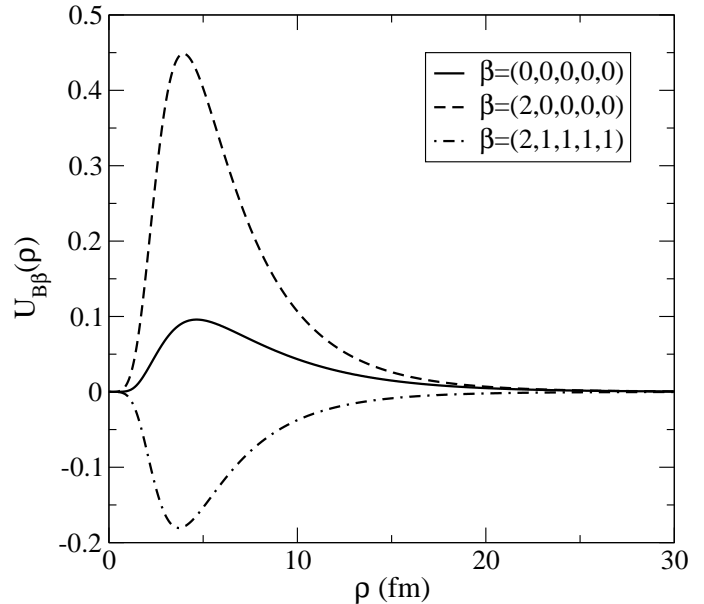


Figure 2: Radial part for the dominant components of the ${}^6\text{He}$ ground state wavefunction. The labels stand for the angular momentum quantum numbers, in the order (K, l_x, l_y, l, S)

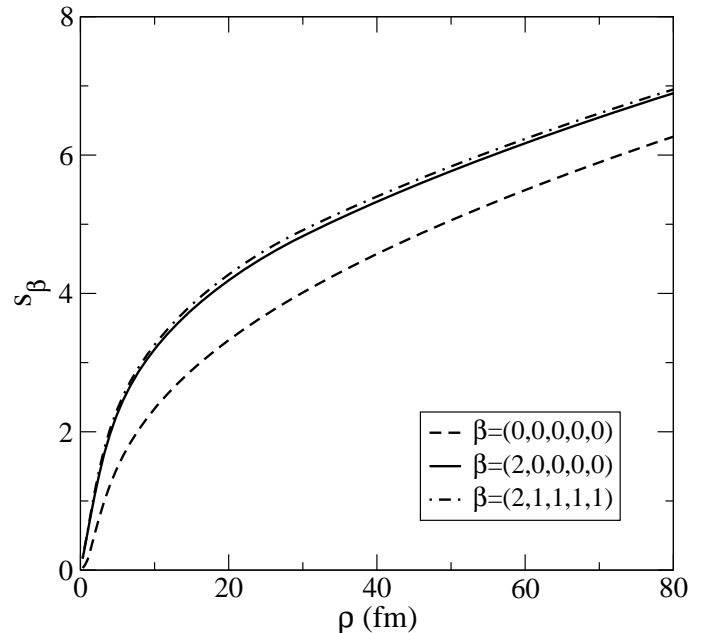


Figure 3: Local scale transformations for the first three channels included in ${}^6\text{He}$ ground state wavefunction.

from the information we have for the ground state. Close to the origin the hyperradial wave functions behave as ρ^K . Thus, in order to calculate the LST for states with $J = 2$ and hypermomentum K ($K = 2, 4, 6, \dots, 2n$) we use the ground state component with $J = 0$ and the same value for K (and also l_x, l_y, l, S if needed). Again, using the LST we generate the basis for $J = 2$ and diagonalize

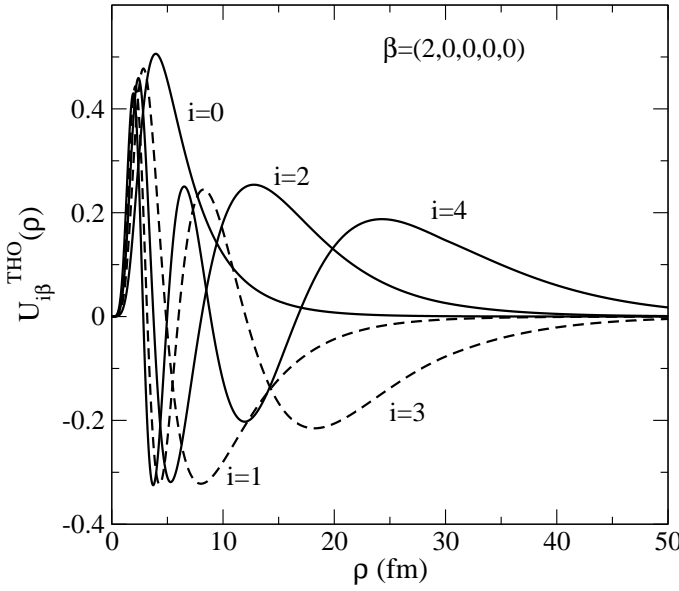


Figure 4: First five THO states for the $J = 0$ channel $\beta = \{2, 0, 0, 0, 0\}$.

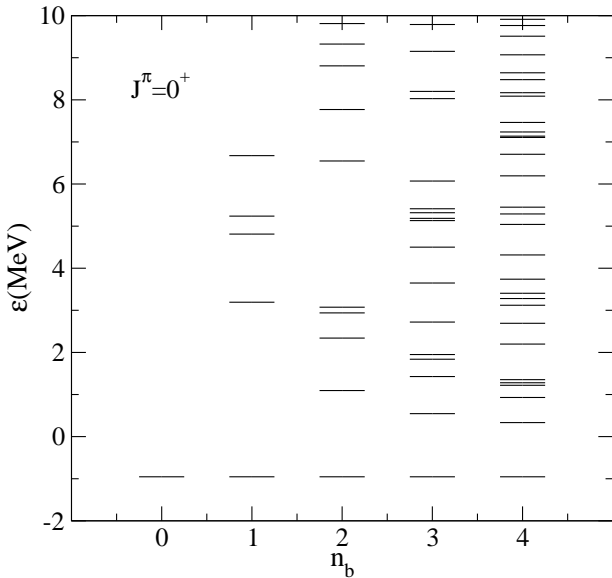


Figure 5: Eigenvalues of $J^\pi = 0^+$ states below $\varepsilon = 10$ MeV.

the Hamiltonian.

In Fig. 6, the eigenvalues of the Hamiltonian for $J^\pi = 2^+$ states are presented for different values of n_b . Again the lowest state is very stable and is close to the energy of the known 2^+ resonance, that is 0.824 MeV. The states with $J = 1$ have odd K ($K = 1, 3, 5, \dots, 2n-1$). Since the ground state wave function contains only even K , for the generation of the LST for the $J = 1$ state we have taken the ground state component with $K - 1$ and multiplied this by ρ , to recover the correct behaviour close to the origin. To select different channels with the same value for K we look for coincidence in l_x, l_y, l, S . Again, from the LST we generate the basis for $J = 1$ and diagonalize

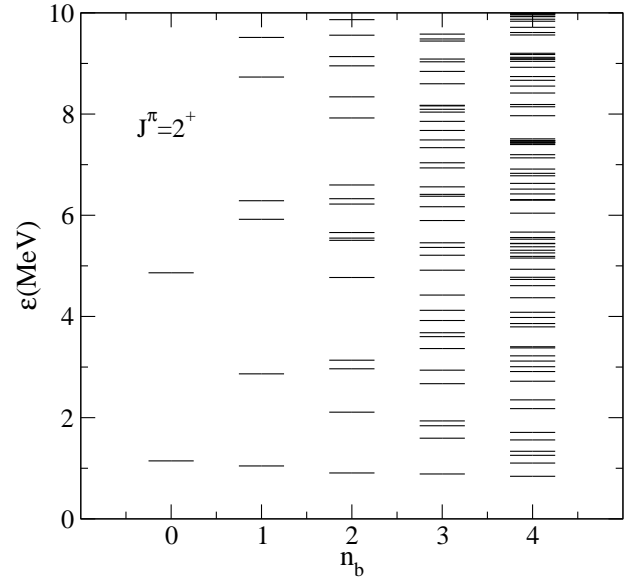


Figure 6: Eigenvalues of $J^\pi = 2^+$ states below $\varepsilon = 10$ MeV.

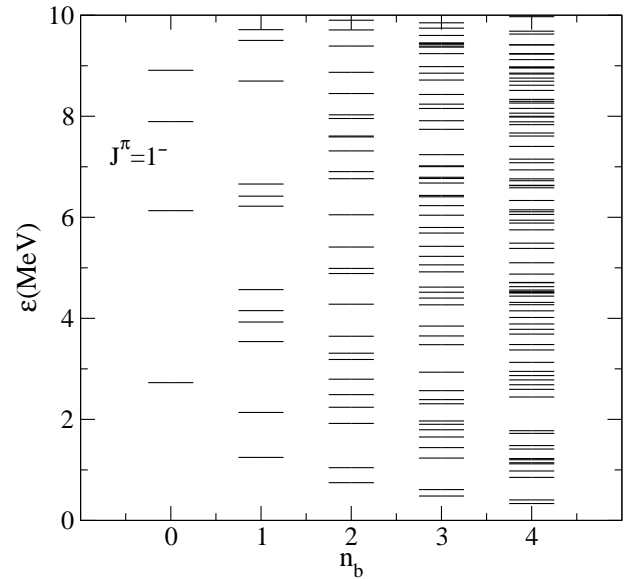


Figure 7: Eigenvalues of $J = 1^-$ states below $\varepsilon = 10$ MeV.

the Hamiltonian.

In Fig. 7, the eigenvalues of the Hamiltonian for $J^\pi = 1^-$ states are presented for different values of n_b . We now see that the lowest state changes as a function of n_b , and goes down in energy as the dimension of the basis is increased.

We now calculate response functions of our system and assess their convergence with the dimension of our truncation of the THO basis.

A. Completeness

In general, a pseudostate with energy ε_n will be a superposition of the actual continuum states nearby in en-

ergy. There are different ways of assigning an energy distribution to a pseudostate [6, 7, 40]. Here we propose a method that takes as reference a large basis with $N_t = (N_b + 1) \times N_{chan}$ states, where N_b is the number of hyperradial excitations of the large basis and N_{chan} is the number of channels for a given J^π . This basis is considered to be complete for the problem under study. In this basis an energy distribution $f_N(\varepsilon, \varepsilon_N)$ is assigned to each discrete state ($N = 1, \dots, N_t$). The width of the distribution is an increasing function of the energy and the distribution can be Gaussian, Lorentzian, or Poisson, etc. We then consider a smaller basis, with $n_t \ll N_t$ states, $n_t = (n_b + 1) \times N_{chan}$, where n_b is the number of hyperradial excitations of the smaller basis. These states n ($n = 1, \dots, n_t$) can be expanded in the large basis

$$|n\rangle = \sum_N C(n, N) |N\rangle. \quad (25)$$

Then, the distribution for the states in the small basis $f_n(\varepsilon, \varepsilon_n)$ is

$$\begin{aligned} f_n(\varepsilon, \varepsilon_n) &= |\langle \varepsilon | n \rangle|^2 = \sum_{NN'} \langle N | \varepsilon \rangle \langle \varepsilon | N' \rangle C(n, N) C(n, N')^* \\ &\approx \sum_N |\langle \varepsilon | N \rangle|^2 |C(n, N)|^2 \\ &= \sum_N f_N(\varepsilon, \varepsilon_N) |C(n, N)|^2. \end{aligned} \quad (26)$$

where we have considered that the off-diagonal terms are small compared with the diagonal terms in the bigger basis.

We have approximated the $f_N(\varepsilon, \varepsilon_N)$ by a Poisson distribution

$$P(\varepsilon, \varepsilon_N, m) = \frac{(m+1)^{(m+1)}}{\varepsilon_N^{(m+1)} m!} \varepsilon^m \exp\left(-\frac{m+1}{\varepsilon_N} \varepsilon\right), \quad (27)$$

which has a width given by

$$\Gamma_N = \sqrt{\langle \varepsilon^2 \rangle - \langle \varepsilon \rangle^2} = \frac{\varepsilon_N}{\sqrt{m+1}}. \quad (28)$$

The larger the value selected for m the narrower the distribution is.

In Figs. 8 and 9 we present the completeness of the large basis to describe states with $J^\pi = 1^-$ and $J^\pi = 2^+$ respectively. The completeness $F(\varepsilon)$ is defined as the sum over all the excited states of $P(\varepsilon, \varepsilon_N, m)$. For the $B(E1)$ distribution a value of $m = 20$ was used. For the $B(E2)$ the same value of m was used except for the region around the resonance for which a value $m = 1300$ had to be used in order to get a width consistent with the experimental value. It is observed that the basis is particularly suited for describing effects in the low lying continuum in both cases.

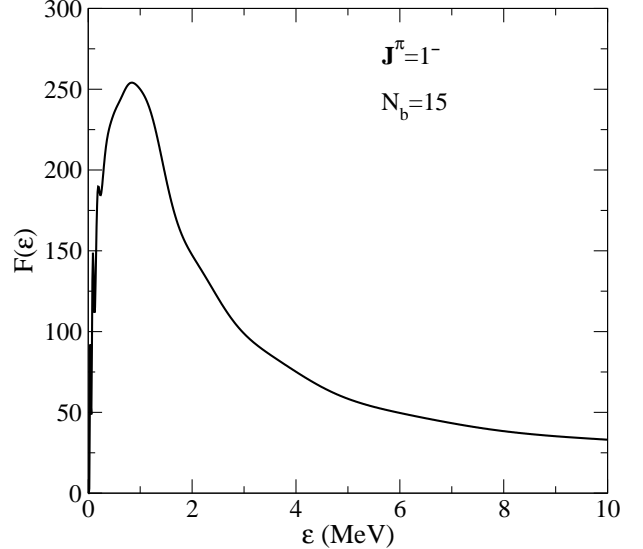


Figure 8: Completeness of the basis with $N_b = 15$ and a Poisson distribution with $m = 20$ for the $J^\pi = 1^-$ states.

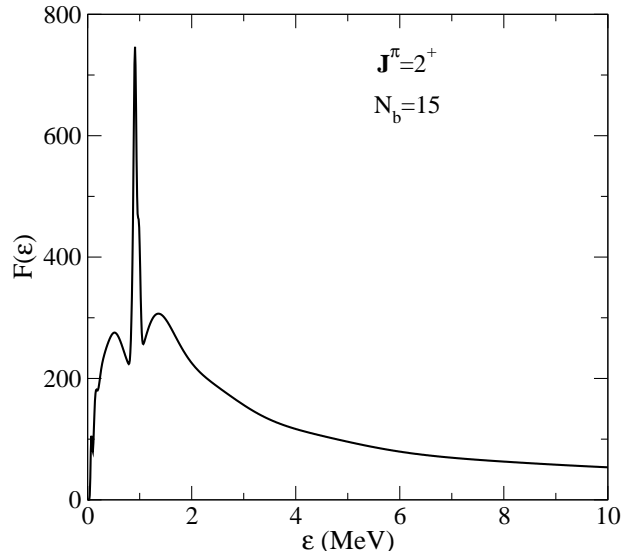


Figure 9: Completeness of the basis with $N_b = 15$ and a Poisson distribution for the $J = 2^+$ states. See text for details on the m values used.

B. Strength functions

To study the effectiveness of the THO basis we start with global observables related to structure, the strength functions. For a given operator \hat{O} , which couples the ground state ($n = 1, J^\pi = 0^+$) with excited states with angular momentum J^π , the following observables are defined:

- Total strength

$$S_T(\hat{O}, n_t) = \sum_n^{n_t} |\langle nJ | \hat{O} | 10 \rangle|^2 \quad (29)$$

where n runs over all the excited states with total

Table I: Convergence of different observables as the THO basis is increased: calculated ground state energy (e_B), expectation value in the ground state for ρ^2 ($\langle \rho^2 \rangle_B$), total strength from the ground state (S_T) [this column should converge to the column labelled $\langle \rho^4 \rangle_B - \langle \rho^2 \rangle_B^2$ according to the sum rule], the ratio between the energy weighted sum and the total strength ($\langle E(n_t) \rangle$) and the ratio between the polarizability and the total strength ($\langle E^{-1}(n_t) \rangle$).

n_b	e_B (MeV)	$\langle \rho^2 \rangle_B$ (fm 2)	S_T (fm 4)	$\langle \rho^4 \rangle_B - \langle \rho^2 \rangle_B^2$ (fm 4)	$\langle E \rangle$ (MeV)	$\langle E^{-1} \rangle$ (MeV $^{-1}$)
0	-0.954882	30.63	41.6	855	27.8	0.0433
1	-0.954884	30.60	738	853	5.72	0.194
2	-0.954885	30.62	851	856	3.08	0.364
3	-0.954885	30.62	855	855	3.01	0.426
4	-0.954886	30.62	854	854	3.00	0.433

angular momentum J^π , up to $n_t = (n_b + 1) \times N_{chan}$. In the limit of a very large number of states n_t , the sum rule for the total strength is

$$S_T(\hat{O}) = \lim_{n_t \rightarrow \infty} S_T(\hat{O}, n_t) = \langle 10 | \hat{O}^2 | 10 \rangle - |\langle 10 | \hat{O} | 10 \rangle|^2. \quad (30)$$

- Energy weighted sum

$$E_w(\hat{O}, n_t) = \sum_n^{n_t} (\varepsilon_{nJ} - \varepsilon_{10}) |\langle nJ | \hat{O} | 10 \rangle|^2. \quad (31)$$

- Polarizability

$$\alpha(\hat{O}, n_t) = \sum_n^{n_t} (\varepsilon_{nJ} - \varepsilon_{10})^{-1} |\langle nJ | \hat{O} | 10 \rangle|^2. \quad (32)$$

In Table I we present the results for the case $\hat{O} = \rho^2$ that connects the ground state with the excited states with $J^\pi = 0^+$. This calculation is performed with $K_{max} = 20$ and different values of n_b .

Note that, already for $n_b = 2$, the total strength acquires a value which is very close to the sum rule value. This indicates that the THO basis is very efficient to describe the ground state through the relatively long range monopole operator ρ^2 . The values of $\langle E(n_t) \rangle$ and $\langle E^{-1}(n_t) \rangle$ also stabilize for low values of n_b and indicate the range of energies in the continuum which are relevant. In our case, for $J^\pi = 0^+$, it corresponds to low energies of around 3 MeV excitation energy above the break-up threshold.

C. $\mathbf{B(E\lambda)}$ sum rules

We will follow the notations and definitions of Brink and Satchler [41]. The electric multipole operator

Table II: Convergence of observables as a function of the dimension (n_b) of the basis considered. The observables presented are: the total strength for $\mathbf{B(E1)}$ excitations from the ground state ($\sum_n B(E1)_{10,n1}$), the energy weighted sum (E_w), the ratio between these magnitudes ($\langle E \rangle = E_w / \sum_n B(E1)_{10,n1}$) and the polarizability (α) below $\varepsilon = 10$ MeV.

n_b	$\sum_n B(E1)_{10,n1}$ (e 2 fm 2)	E_w (e 2 fm 2 MeV)	$\langle E \rangle$ (MeV)	α (e 2 fm 2 MeV $^{-1}$)
0	1.297	5.38	4.15	0.422
1	1.323	5.71	4.32	0.403
2	1.323	5.76	4.36	0.403
3	1.321	5.76	4.36	0.402
4	1.320	5.75	4.35	0.402

Table III: Same as Table II but for E2 transitions.

n_b	$\sum_n B(E2)_{10,n2}$ (e 2 fm 4)	E_w (e 2 fm 4 MeV)	$\langle E \rangle$ (MeV)	α (e 2 fm 4 MeV $^{-1}$)
0	3.51	14.5	4.09	1.21
1	6.89	27.6	4.01	2.37
2	8.41	31.1	3.70	3.06
3	8.47	30.5	3.60	3.20
4	8.41	30.1	3.58	3.19

$Q_{\lambda M_\lambda}(\mathbf{r})$ is defined as

$$Q_{\lambda M_\lambda}(\mathbf{r}) = \left(\frac{4\pi}{2\lambda + 1} \right)^{1/2} Z e r^\lambda Y_{\lambda M_\lambda}(\hat{r}), \quad (33)$$

where e is the electron charge and Z is the atomic number of the system. For a nucleus with a core plus two valence neutrons, $\mathbf{r} = \mathbf{y} \sqrt{m \mu_y} / m_c$ is the position of the core (charged particle) relative to the center of mass of the system. m_c is the mass of the core. For ${}^6\text{He}$, $Z = 2$ and $\mathbf{r} = \mathbf{y} / (2\sqrt{3})$, as presented in Fig. 1. The reduced transition probability is

$$B(E\lambda)_{nJ, n'J'} \equiv B(E\lambda; nJ \rightarrow n'J') = |\langle nJ | Q_\lambda | n'J' \rangle|^2 \left(\frac{2\lambda + 1}{4\pi} \right) \quad (34)$$

where the reduced matrix element $\langle nJ | Q_\lambda | n'J' \rangle$ is defined as

$$\langle nJM | Q_{\lambda M_\lambda} | n'J'M' \rangle = (-1)^{2\lambda} \langle J'M' \lambda M_\lambda | JM \rangle \times \langle nJ | Q_\lambda | n'J' \rangle. \quad (35)$$

Using some angular momentum algebra we arrive to the final expression

$$\begin{aligned}
B(E\lambda)_{nJ,n'J'} &= \frac{2\lambda+1}{4\pi} |\langle nJ || Q_\lambda || n'J' \rangle|^2 \\
&= \frac{(2\lambda+1)(2J'+1)}{4\pi} Z^2 e^2 \left(\frac{\sqrt{m\mu_y}}{m_c} \right)^{2\lambda} \\
&\times \left| \sum_{\beta\beta'} \delta_{SS'} \delta_{l_x l'_x} \sum_{ii'} C_n^{i\beta} C_{n'}^{i'\beta'} \hat{l} \hat{l}' \hat{l}_y \hat{l}'_y (-)^{l_x+S} \right. \\
&\times \left(\begin{array}{ccc} l_y & \lambda & l'_y \\ 0 & 0 & 0 \end{array} \right) W(l l' l_y l'_y; \lambda l_x) W(J J' l l'; \lambda S) \\
&\times \left. \int \int (\sin \alpha)^2 (\cos \alpha)^2 d\alpha d\rho y^\lambda U_{i\beta}^{THO}(\rho) \Psi_K^{l_x l_y}(\alpha) \Psi_{K'}^{l_x l_y}(\alpha) U_{i'\beta'}^{THO}(\rho) \right|^2. \quad (36)
\end{aligned}$$

Using this expression it is simple to calculate the sum rules of electric transitions from the ground state, $n = 1$, $J^\pi = 0^+$, to the states (n, J) : $\sum_n B(E\lambda)_{10,nJ}$,

$$\sum_n B(E\lambda)_{10,nJ} = \left(\frac{2\lambda+1}{4\pi} \right) \sum_n |\langle 1 0 || Q_\lambda || nJ \rangle|^2. \quad (37)$$

In particular, we are interested in the $\lambda = 1$ electric dipole strength, connecting the $J^\pi = 0^+$ ground state to the $J^\pi = 1^-$ states, and in the $\lambda = 2$ electric quadrupole strength, connecting the ground state to the $J^\pi = 2^+$ states:

• B(E1) sum rule

$$\sum_n B(E1)_{10,n1} = \frac{3}{4\pi} \frac{Z^2 e^2 m \mu_y}{m_c^2} \langle 1 0 | y^2 | 1 0 \rangle. \quad (38)$$

• B(E2) sum rule

$$\sum_n B(E2)_{10,n2} = \frac{5}{4\pi} \frac{Z^2 e^2 m^2 \mu_y^2}{m_c^4} \langle 1 0 | y^4 | 1 0 \rangle. \quad (39)$$

Tables II and III show the results obtained for ${}^6\text{He}$ when including states up to 10 MeV in excitation energy above the two-neutron break-up threshold. These include the $B(E\lambda)$, total strength, energy weighted sum, and polarizability. The $B(E1)$ and $B(E2)$ sum rule values for the total strength are $1.500 \text{ e}^2 \text{fm}^2$ and $9.99 \text{ e}^2 \text{fm}^4$, respectively. The values in the second column in Tables II and III are close to these limits but do not reach them since only states up to 10 MeV are included. If the complete sum is done the values are $1.498 \text{ e}^2 \text{fm}^2$ and $9.59 \text{ e}^2 \text{fm}^4$ that are close to the corresponding sum rule values.

D. B(E1) and B(E2) distributions

To obtain a continuous $B(E\lambda)$ distribution from the discrete values $B(E\lambda)_{10,nJ}$ we can apply the procedure described in subsection III A. In this case we have to evaluate

$$\begin{aligned}
|\langle gs | \hat{O} | \varepsilon \rangle|^2 &= \langle gs | \hat{O} | \varepsilon \rangle \langle \varepsilon | \hat{O} | gs \rangle \approx \sum_{nn'} \langle gs | \hat{O} | n \rangle \langle n | \varepsilon \rangle \langle \varepsilon | n' \rangle \langle n' | \hat{O} | gs \rangle \\
&= \sum_{nn'} \langle gs | \hat{O} | n \rangle \langle n' | \hat{O} | gs \rangle \sum_{NN'} \langle N | \varepsilon \rangle \langle \varepsilon | N' \rangle C(n, N) C(n', N')^* \\
&\approx \sum_{nn'} \langle gs | \hat{O} | n \rangle \langle n' | \hat{O} | gs \rangle \sum_N C(n, N) f_N(\varepsilon, \varepsilon_N) C(n', N)^* \\
&= \sum_N f_N(\varepsilon, \varepsilon_N) SO(N) SO(N)^* \quad (40)
\end{aligned}$$

where $SO(N) = \sum_n \langle gs | \hat{O} | n \rangle C(n, N)$. We have used this method to calculate $B(E\lambda)$ distributions. For this pur-

pose we have taken a large basis with $N_t = (N_b + 1) \times N_{chan}$ states, where $N_b = 15$. The Poisson distribution

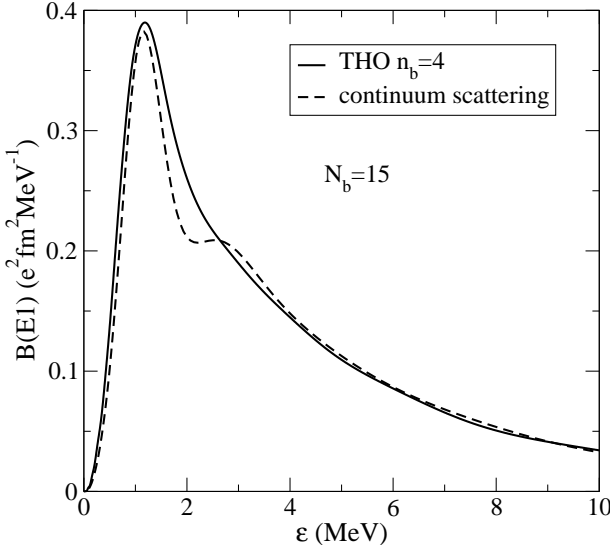


Figure 10: $B(E1)$ distribution for $n_b = 4$ with $n_t = (n_b + 1) \times N_{chan}$ and a Poisson distribution with $m = 20$.

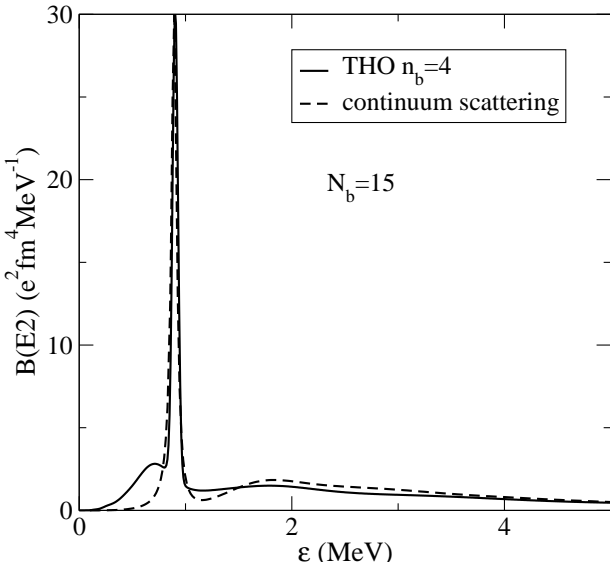


Figure 11: $B(E2)$ distribution for $n_b = 4$ with $n_t = (n_b + 1) \times N_{chan}$ and a Poisson distribution with $m = 20$.

used had $m = 20$.

In Figs. 10 and 11 we present the $B(E1)$ and $B(E2)$ distributions up to 10 MeV. Calculations for different dimensions of the THO basis are not presented, but are practically indistinguishable. For comparison, the distribution calculated with the continuum scattering wave functions is also shown. The latter is the calculation reported in Ref. [38]. For the $B(E1)$ the distributions are in good agreement with the maximum at around 1.2 MeV and with the same total strength. For the $B(E2)$ distributions the most relevant feature is the appearance of a narrow low-lying resonance. In both calculations the depth of the three-body interaction was adjusted to reproduce the position of the 2^+ resonance at 0.824 MeV. Again we find good agreement between the calculations

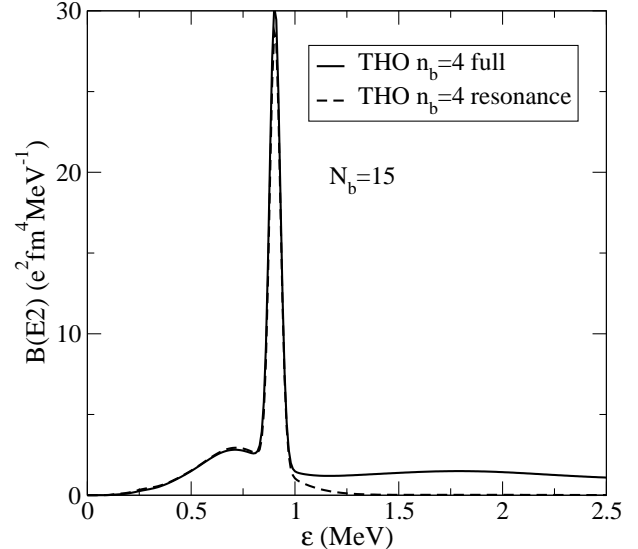


Figure 12: Total $B(E2)$ distribution for $n_b = 4$ and resonance $B(E2)$ distribution for $n_b = 4$ and for a Poisson distribution with $m = 20$.

in both shape and total strength. As noted above, we used a larger m value for the energy region around the resonance. Our calculations exhibit a small bump just below the resonance which does not appear in the continuum scattering calculation. This small difference comes from the low energy components of the resonance. This is more clearly shown in Fig. 12 where, besides the full $B(E2)$ distribution, we have superimposed the contribution of the first $J^\pi = 2^+$ state that appears around the resonance energy in the THO calculation for $n_b = 4$. This single state reproduces the resonant peak very well.

IV. SUMMARY AND CONCLUSIONS

We have presented a generalization of the transformed harmonic oscillator (THO) method proposed in [13] appropriate for three-body problems. The method provides a discrete representation of the continuum spectrum of a three-body system from a knowledge of its ground state wave function, either in analytical or numerical form. This wave function is used to obtain a local scale transformation that converts this state into a harmonic oscillator ground state. The inverse transformation is then applied to the corresponding excited harmonic oscillator states to obtain a basis set for the physical system. Finally, the three-body Hamiltonian is diagonalized in this basis, providing a discrete representation of eigenstates and eigenvalues of the three-body system.

The formalism has been applied here to the Borromean nucleus ${}^6\text{He}$, for which several strength functions, including the dipole and quadrupole Coulomb transition strengths, have been calculated. These observables are found to converge quickly with respect to the number of THO basis states included. Furthermore, the calculated

strength distributions are in very good agreement with previous results obtained using a three-body continuum scattering wave functions. The results found in this work suggest that the THO basis could also be effective for continuum discretization in scattering calculations. Work in this direction is in progress and results will be presented in a future publication.

FPA2002-04181-C04-04 and in part by EPSRC under grant GR/M82141. A.M.M. acknowledges a research grant from the Junta de Andalucía. M.R.G. acknowledges a research grant from the Ministerio de Educación and the Marie Curie Training Site. Enlightening discussions with Prof. R. C. Johnson are deeply acknowledged.

Acknowledgments

This work was supported in part by the Spanish DGICYT under project numbers BFM2002-03315 and

[1] P. G. Hansen, A. Jensen, and B. Jonson, *Ann. Rev. Nucl. Part. Sci.* **45**, 591 (1995).

[2] A. S. Jensen, D. V. Riisager, K. Fedorov, and E. Garrido, *Rev. Mod. Phys.* **76**, 215 (2004).

[3] M. Yahiro, Y. Iseri, H. Kameyama, M. Kamimura, and M. Kawai, *Prog. Theor. Phys. Suppl.* **89**, 32 (1986).

[4] N. Austern, Y. Iseri, M. Kamimura, M. Kawai, G. Rawitscher, and M. Yahiro, *Phys. Rep.* **154**, 125 (1987).

[5] T. Matsumoto *et al.*, *Phys. Rev. C* **68**, 064607 (2003).

[6] A. Macías, F. Martín, and M. Yáñez, *Phys. Rev. A* **36**, 4179 (1987).

[7] I. Bray, *Comp. Phys. Comm.* **85**, 1 (1995).

[8] Z. C. Kuruoglu and F. S. Levin, *Phys. Rev. Lett.* **48**, 899 (1982).

[9] Z. Kuruoglu, *Phys. Rev. C* **43**, 1061 (1991).

[10] E. Hiyama, Y. Kino, and M. Kamimura, *Prog. Part. Nucl. Phys.* **51**, 223 (2003).

[11] T. Matsumoto *et al.*, *Phys. Rev. C* **70**, 061601 (2004).

[12] I. Petkov and M. Stoitsov, *C.R. Acad. Bulg. Sci.* **34**, 1651 (1981).

[13] F. Pérez-Bernal, I. Martel, J. M. Arias, and J. Gómez-Camacho, *Phys. Rev. A* **63**, 052111 (2001).

[14] F. Pérez-Bernal, I. Martel, J. M. Arias, and J. Gómez-Camacho, *Few Body Sys. Suppl.* **13**, 213 (2001).

[15] M. Rodríguez-Gallardo, J. M. Arias, and J. Gómez-Camacho, *Phys. Rev. C* **69**, 034308 (2004).

[16] A. M. Moro, J. M. Arias, J. Gómez-Camacho, I. Martel, F. Pérez-Bernal, F. Nunes, and R. Crespo, *Phys. Rev. C* **65**, 011602 (2002).

[17] I. Martel, F. Pérez-Bernal, M. Rodríguez-Gallardo, J. M. Arias, and J. Gómez-Camacho, *Phys. Rev. A* **65**, 052708 (2002).

[18] F. Aksough *et al.*, *Review of the University of Milano, Ricerca Scientifica ed educazione permanente Suppl.* **122** (2003).

[19] P. Egelhof, *Nucl. Phys. A* **722**, C254 (2002).

[20] T. Aumann, L. V. Chulkov, V. N. Pribora, and M. H. Smedberg, *Nucl. Phys. A* **640**, 24 (1998).

[21] T. Aumann *et al.*, *Phys. Rev. C* **59**, 1252 (1999).

[22] E. F. Aguilera *et al.*, *Phys. Rev. C* **63**, 061603 (2001).

[23] E. F. Aguilera *et al.*, *Phys. Rev. Lett.* **84**, 5058 (2000).

[24] O. R. Kakuee *et al.*, *Nucl. Phys. A* **728**, 339 (2003).

[25] M. V. Zhukov, B. V. Danilin, D. V. Fedorov, J. M. Bang, I. J. Thompson, and J. S. Vaagen, *Physics Reports* **231**, 151 (1993).

[26] E. Hiyama and M. Kamimura, *Nucl. Phys. A* **588**, 35c (1995).

[27] B. V. Danilin, T. Rogde, S. N. Ershov, H. Heiberg-Andersen, J. S. Vaagen, I. J. Thompson, and M. V. Zhukov, *Phys. Rev. C* **55**, R577 (1997).

[28] D. V. Fedorov, E. Garrido, and A. S. Jensen, *Few Body Syst.* **33**, 153 (2003).

[29] E. Garrido, D. V. Fedorov, A. S. Jensen, and H. O. U. Fynbo, *Nucl. Phys. A* **748**, 39 (2005).

[30] T. Myo, K. Kato, S. Aoyama, and K. Ikeda, *Phys. Rev. C* **63**, 054313 (2001).

[31] Y. Suzuki, *Nucl. Phys. A* **528**, 395 (1991).

[32] S. Funada, H. Kameyama, and Y. Sakuragi, *Nucl. Phys. A* **575**, 93 (1994).

[33] P. Navratil and B. R. Barrett, *Phys. Rev. C* **54**, 2986 (1996).

[34] A. Csótó, *Phys. Rev. C* **48**, 165 (1993).

[35] J. Wurzer and H. M. Hofmann, *Phys. Rev. C* **55**, 688 (1997).

[36] I. J. Thompson, F. M. Nunes, and B. V. Danilin, *Comput. Phys. Commun.* **161**, 87 (2004).

[37] J. Bang and C. Gignoux, *Nucl. Phys. A* **313**, 119 (1979).

[38] I. J. Thompson, B. V. Danilin, V. D. Efros, J. S. Vaagen, J. M. Bang, and M. V. Zhukov, *Phys. Rev. C* **61**, 24318 (2000).

[39] D. Gogny, P. Pires, and R. de Tourreil, *Phys. Lett.* **32B**, 591 (1970).

[40] R. Crespo, I. J. Thompson, and A. A. Korsheninnikov, *Phys. Rev. C* **66**, 021002 (2002).

[41] D. M. Brink and G. R. Satchler, *Angular Momentum* (Clarendon, Oxford, 1994).